A Gas-Solid Reaction with Nonuniform Distribution of Solid Reactant

A pore-pellet model is used to analyze experimental data for SO_2 removal using CuO impregnated on alumina as a sorbent. The effect of structural changes in the active solid (CuO) is included in the analysis and found to be important. The changes are characterized by three parameters: the ratio of solid product ($CuSO_4$) molal volume to solid reactant (CuO) molal volume, the weight fraction of active solid, and the radial distribution of the active solid within the pellet.

The calculated kinetic constants are independent of CuO weight fraction and can be used for pellets with different CuO weight fractions. For the data set used in this work, it is shown that some degree of nonuniformity in the CuO distribution within the alumina matrix is needed in order to obtain a good fit of the data by the model.

C. G. Dassori
J. W. Tierney
Y. T. Shah
Department of Chemical and Petroleum Engineering
University of Pittsburgh
Pittsburgh, PA 15261

Introduction

Noncatalytic gas-solid reactions have been examined extensively in the literature and have been the subject of recent reviews by Ramachandran and Doraiswamy (1982) and Doraiswamy and Sharma (1984). This interest is due to their many practical applications, such as in the reduction of certain ores, removal of gaseous pollutants (flue gas desulfurization), coal gasification, and regeneration of coked catalysts. Recently, attention has been focused on the role in the reaction process of nonuniform solid reactant distribution over an inert material (Dudukovic, 1984; Ramachandran and Dudukovic, 1984; Sohn and Xia, 1986, 1987). These studies have established the importance of initial solid reactant distribution on the solid conversion-time relationship for nonporous and porous solids, with no structural changes during the course of reaction.

Recent work by Prasannan et al. (1985) evaluated the effect of different weight fractions of active solid on an inert matrix on the performance of gas-solid reactions in the presence of structural changes. The analysis was based on the particle-pellet model and the role of pore closure on total gas uptake was studied, assuming uniform active solid distribution.

The objecive of this paper is to present a model for gas-solid reactions that allows for possible structural changes during the course of reaction, and that provides for an arbitrary initial active solid distribution on an inert matrix. In this way, the analysis combines different approaches attempted so far and provides a means to obtain kinetic constants that are not affected by the way in which the solid reactant is distributed over the inert support or by the value of the active solid weight fraction. This also requires more information about the solid structure of the pellet. For a case study the model is applied to SO_2 removal using CuO impregnated on alumina as a sorbent.

The Model

Development

The solid pellet is considered to be an assembly of pores embedded in a porous solid matrix of inert material. After this matrix is impregnated by the active solid, the gaseous reactant diffuses through the pores of the pellet and reacts with the active solid that covers the inert matrix.

We consider a reaction represented by:

$$A(g) + bB(s) = gG(s) + P(g)$$

where B is the solid reactant. It has been found that SO_2 absorption on CuO fits this type of equation (Yeh et al., 1982). As the reaction proceeds a layer of porous solid G grows over the surface of the active pores. Due to differences in stoichiometric coefficients and in molal densities of the product and reactant, the void volume of the pores grows or shrinks. Diffusivity varies as the porosity changes. It is assumed that:

1. The radius of the pellet does not change during reaction
2. The pore shape is cylindrical, Figure 1, and the reacting pores retain their shape during the course of reaction

The present address of C. G. Dassori and Y. T. Shah is University of Tulsa, College of Engineering and Applied Sciences, Tulsa, OK 74104.

3. The reaction is isothermal and sintering does not occur
4. The number of pores in a pellet remains constant during the course of reaction and is the same as for the initial inert matrix
5. The net mass flux can be neglected—valid if the concentration of A is very small or if gases A and P are undergoing equimolar counterdiffusion
6. The reaction is first order with respect to both the gaseous reactant concentration and the reactive solid surface. Here it is implied that the reaction takes place at a sharp interface between the nonporous reactant and the porous product layer within the active pores.

Some of the above assumptions deserve discussion. The size of the pellet generally remains unchanged during the course of the reaction, particularly if the major part of the pellet is inert. SO_2 removal using CuO as a sorbent is usually carried out with less than 10 wt. % Cu in the pellet. The assumption of a cylindrical pore shape is more arbitrary. Nevertheless, a number of researchers have used this assumption, and the consideration of more general geometries for the pore shape would imply a deeper insight into the structure of the solid and a higher level of information than are currently available. We consider a cylindrical shape and a uniform size distribution for the pores. The assumption of retention of pore shape during reaction seems appropriate if the active solid is impregnated over an inert matrix. In the absence of a solid inert support this assumption would be more difficult to justify. The inert matrix also makes it more likely that the number of pores per unit volume of pellet will not change. It is assumed that the temperature is not high enough to cause sintering. However, if present, sintering could contribute substantially to structural changes during reaction (Ramachandran and Smith, 1977; Dassori et al., 1987). For SO_2 removal with CuO, the usual range of temperature employed, 350–450°C, makes it unnecessary to consider sintering.

Model formulation

We denote by r_o the radius of the pores, Figure 1, in the initial inert matrix and their length by ℓ. The initial macroporosity, ϵ^*, and the initial surface area per unit pellet volume (before impregnation), S_i, can be related to r_o, ℓ, and N_p (the number of pores per unit volume) by the expressions:

$$\epsilon^* = \pi r_o^2 N_p \ell \tag{1}$$

$$S_i = 2\pi r_o N_p \ell \tag{2}$$

After the process of impregnation has been completed, we assume that the number of pores per unit volume remains the same. The active solid is distributed along the radius of the pellet with an active to inert solid weight ratio, W, so that the volume-averaged value of this function is $\overline{W}$. We also consider that the active solid covers a fraction, $f_a(r)$, of the inert support surface area, where r means dependence on the radial direction within the pellet. To account for the surface coverage, we assume that this fraction $f_a(r)$ can be related to the fraction of pores covered by active solid, $f_p(r)$.

If $\zeta(r)$ is the thickness of the active solid layer covering the pores, f_a is related to f_p by the expression:

$$f_a = \frac{f_p(1 - \zeta/r_o)}{1 - f_p\zeta/r_o} \tag{3}$$

where f_a and f_p are subject to the constraints:

$$0 \le f_a \le 1 \tag{4}$$

$$0 \le f_p \le 1 \tag{5}$$

The active to inert solid weight ratio, W, can be written as:

$$W(r) = \frac{\epsilon^* - \epsilon^o(r)}{1 - \epsilon^*}\frac{\rho_B}{\rho_i} \tag{6}$$

where ρ_B and ρ_i are the solid densities of active solid B and inert material, respectively, and $\epsilon^o(r)$ is the local porosity at the r position within the pellet. Equation 6 can be volume-averaged as:

$$\overline{W} = \frac{3}{R_p^3}\int_o^{R_p} r^2 \frac{\epsilon^* - \epsilon^o}{1 - \epsilon^*}\frac{\rho_B}{\rho_i}\,dr \tag{7}$$

where R_p is the pellet radius. In addition W is chosen so that:

$$\overline{W} = \frac{3}{R_p^3}\int_o^{R_p} r^2 W dr \tag{8}$$

$\overline{W}$, the volume-averaged value of W, can be related to the global weight fraction of the active solid, $\overline{W}_f$, through:

$$\overline{W} = \frac{\overline{W}_f}{1 - \overline{W}_f} \tag{9}$$

The porosity, ϵ^o, and surface area, S^o, at the initial time of reaction can be written as follows:

$$\epsilon^o = \epsilon^*[(1 - \zeta/r_o)^2 f_p + 1 - f_p] \tag{10}$$

$$S^o = S_i[(1 - \zeta/r_o) f_p + 1 - f_p] \tag{11}$$

We can substitute Eq. 10 into Eq. 6 to obtain:

$$W = \frac{\epsilon^* - \epsilon^*[(1 - \zeta/r_o)^2 f_p + 1 - f_p]}{1 - \epsilon^*}\frac{\rho_B}{\rho_i} \tag{12}$$

Now Eq. 12 can be examined for two special cases. First, for complete coverage of the internal surface of the inert support ($f_a = f_p = 1$ for all radial positions), Eq. 12 reduces to:

$$W = \frac{\epsilon^* - \epsilon^*(1 - \zeta/r_o)^2}{1 - \epsilon^*}\frac{\rho_B}{\rho_i} \tag{13}$$

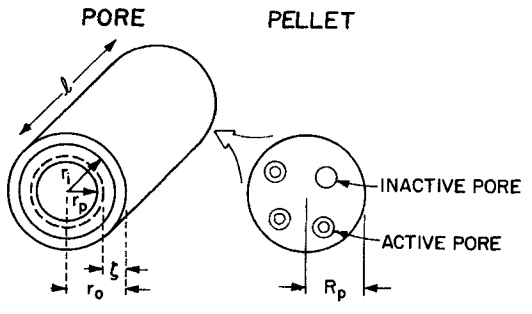

Figure 1. Representations of pore and pellet for model.

and we can obtain an expression for ζ/r_o as:

$$\zeta/r_o = 1 - \sqrt{1 - \frac{\rho_i}{\rho_B} W \frac{1-\epsilon^*}{\epsilon^*}} \tag{14}$$

Second, for the case of incomplete surface coverage ($f_a < 1$), but for a constant value for ζ/r_o, from Eq. 12 we obtain:

$$f_p = \frac{W \frac{1-\epsilon^*}{\epsilon^*} \frac{\rho_i}{\rho_B}}{1 - (1 - \zeta/r_o)^2} \tag{15}$$

so that once $W(r)$ is fixed and ζ/r_o has a value, f_p can be calculated and then $f_a(r)$ is known from Eq. 3.

The reaction rate per active pore can be obtained by considering both diffusion through the product layer and reaction at a sharp interface of area $2\pi r_i \ell$. The diffusion rate can be expressed as:

$$-\frac{dn_A}{dt} = D_s \frac{A_i - A_p}{\ln\left(\frac{A_i}{A_p}\right)} \frac{C_A - C_{Ai}}{r_i - r_p} \tag{16}$$

with

$$A_i = 2\pi r_i \ell \tag{17}$$

$$A_p = 2\pi r_p \ell \tag{18}$$

whereas using the assumption of Eq. 6, the chemical reaction rate can be expressed as

$$-\frac{dn_A}{dt} = 2\pi r_i \ell k C_{Ai} \tag{19}$$

Eliminating the interfacial concentration, C_{Ai}, the rate of reaction per reacting pore can be expressed as:

$$-\frac{dn_A}{dt} = 2\pi r_i \ell \frac{kC_A}{1 + \frac{kr_i}{D_s} \ln\left(\frac{r_i}{r_p}\right)} \tag{20}$$

In these equations D_s is the effective diffusivity of the gaseous reactant through the product layer; r_i is the radius of the reaction interface; and r_p is the radius of the active reactant pore at any time, Figure 1. The radius r_p is a function of time and radial position in the pellet for those cases where there is structural change in the solid phase. This radius can be expressed in terms of the densities of the reactant and product solids by a mass balance on the product layer as:

$$\frac{1}{g}(\text{moles of } G \text{ formed}) = \frac{1}{b}(\text{moles of } B \text{ reacted})$$

or

$$\frac{\pi\ell}{g}(r_i^2 - r_p^2)\frac{\rho_G}{M_G}(1 - \epsilon_G) = \frac{\pi\ell}{b}\frac{\rho_B}{M_B}[r_i^2 - (r_o - \zeta)^2] \tag{21}$$

which can be finally written as:

$$r_i^2 - r_p^2 = C_v[r_i^2 - (r_o - \zeta)^2] \tag{22}$$

with

$$C_v = \frac{gM_G\rho_B}{bM_B\rho_G(1 - \epsilon_G)} \tag{23}$$

One can obtain the rate per unit volume of the pellet by multiplying the rate per pore, eq. 20, and the number of active pores per unit volume, $N_p f_p$. The mass conservation for A within the macropores of the pellet can be thus formulated as:

$$\frac{1}{r^2}\frac{\partial}{\partial r}\left(D_e r^2 \frac{\partial C_A}{\partial r}\right) - \frac{S_i^2 f_p}{2\epsilon^*} \frac{kC_A r_i}{1 + \frac{kr_i}{D_s}\ln\left(\frac{r_i}{r_p}\right)} = \epsilon \frac{\partial C_A}{\partial t} \tag{24}$$

The rate of change of the position of the reaction interface can be obtained from a mass balance on reactant B as:

$$r_B = N_p f_p \frac{d}{dt}\left(\pi r_i^2 \ell \frac{\rho_B}{M_B}\right) = N_p f_p b\left(-\frac{dn_A}{dt}\right) \tag{25}$$

or

$$\frac{dr_i}{dt} = \frac{M_B b k C_A}{\rho_B\left(1 + \frac{kr_i}{D_s}\ln\left(\frac{r_i}{r_p}\right)\right)} \tag{26}$$

Equations 24 and 26 must be integrated with the following initial and boundary conditions:

$$t = 0, \quad C_A = C_A^* \tag{27}$$

$$r_p = r_i = r_o - \zeta \tag{28}$$

$$r = 0, \quad \partial C_A/\partial r = 0 \tag{29}$$

$$r = R_p, \quad C_A = C_A^o \tag{30}$$

where C_A^o is the bulk gas concentration and C_A^* is the initial gas concentration inside the macropores of the pellet. We have neglected any mass transport resistance in the bulk gas phase.

Structural changes

The structural changes that the solid undergoes as a result of chemical reaction (swelling or shrinkage) cause a change in the effective diffusivity of the gas reactant through the pellet. One simple way to account for this is to use the random pore model (Satterfield, 1970). According to this model the effective diffusivity is given by:

$$D_e = \left(\frac{1}{D_M} + \frac{1}{D_K}\right)^{-1}\epsilon^2 \tag{31}$$

where D_M is the molecular diffusivity of gaseous reactant and D_K is the Knudsen diffusivity. The porosity of the pellet will vary

according to time and radial position and can be predicted by:

$$\epsilon = \epsilon^* \left[f_p \left(\frac{r_p}{r_o} \right)^2 + 1 - f_p \right] \tag{32}$$

While molecular diffusivity is independent of porosity, Knudsen diffusivity can be calculated from the expression provided by Satterfield (1970):

$$D_K = \frac{19{,}400 \sqrt{T/M_A}\,\epsilon}{S} \tag{33}$$

where T is the temperature in K, M_A is the molecular weight of reactant A in g/mol, and S is the surface area per unit volume of pellet in cm^{-1}. S is given by:

$$S = S_i \left(\frac{r_p}{r_o} f_p + 1 - f_p \right) \tag{34}$$

With the solution of the problem one can calculate the fractional conversion of solid B(CuO for the SO_2-CuO process):

$$X_B = \frac{\int_o^{R_p} r^2 f_p [r_i^2 - (r_o - \zeta)^2]\, dr}{\int_o^{R_p} r^2 f_p [r_o^2 - (r_o - \zeta)^2]\, dr} \tag{35}$$

Dimensionless equations

The above set of equations can be written in dimensionless form as:

$$\frac{1}{R^2} \frac{\partial}{\partial R} \left(\delta R^2 \frac{\partial C}{\partial R} \right) - \phi^{*2} \frac{f_p r_i^* C}{1 + \frac{r_i^*}{Bi} \ln \left(\frac{r_i^*}{r_p^*} \right)} = \epsilon N \frac{\partial C}{\partial \theta} \tag{36}$$

$$\frac{dr_i^*}{d\theta} = \frac{C}{1 + \frac{r_i^*}{Bi} \ln \left(\frac{r_i^*}{r_p^*} \right)} \tag{37}$$

with the following initial and boundary conditions:

$$\theta = 0, \quad C = C^* \tag{38}$$

$$r_p^* = r_i^* = 1 - \zeta / r_o \tag{39}$$

$$R = 0, \quad \partial C / \partial R = 0 \tag{40}$$

$$R = 1, \quad C = 1 \tag{41}$$

The nondimensional relation between r_p^* and r_i^* can now be written as:

$$r_p^{*2} = (1 - C_v) r_i^{*2} + C_v (1 - \zeta / r_o)^2 \tag{42}$$

The porosity and surface area can be written in terms of nondimensional variables as:

$$\epsilon = \epsilon^* (f_p r_p^{*2} + 1 - f_p) \tag{43}$$

$$S = S_i (f_p r_p^* + 1 - f_p) \tag{44}$$

These equations along with Eq. 33 can be substituted into Eq. 31 to obtain the effective diffusivity of gas reactant A during the process. In terms of nondimensional variables Eqs. 8 and 35 become:

$$3 \int_o^1 R^2 W'\, dR = 1 \tag{45}$$

$$X_B = \frac{\int_o^1 R^2 f_p [r_i^{*2} - (1 - \zeta / r_o)^2]\, dR}{\int_o^1 R^2 f_p [1 - (1 - \zeta / r_o)^2]\, dR} \tag{46}$$

where nondimensional W' has been obtained by normalizing W with $\overline{W}$.

A criterion for pore plugging is derived from Eq. 42 by imposing $r_p^* > 0$ for $r_i^* = 1$, as:

$$(1 - \zeta / r_o)^2 > \frac{C_v - 1}{C_v} \tag{47}$$

It should be noted that under pore plugging conditions, the model can be criticized because it does not take into account any interaction among the pores, something that should be expected under these circumstances. However, pore plugging is not likely to occur at moderate or low active solid weight fractions, as is the case for SO_2 removal with CuO, and hence pore interactions have not been included.

Method of Solution

We have used the method of lines to solve the problem represented by Eqs. 36 and 37 with the initial and boundary conditions of Eqs. 38–41. Uniform mesh size (with 61 mesh points) was employed for the discretization of the space variable. The LSODE (Hindmarsh, 1980) integrator was used for the integration of the final set of ordinary differential equations, with the relative and absolute error tolerance parameters for all variables being 10^{-4}. Some runs were made with a 10^{-5} value for both error controls, with negligible variations observed for the solid conversion results. The stiff method option and banded Jacobian matrix (internally generated) were specified when using LSODE, as reported in previous work (Johnson and Hindmarsh, 1983; Sohn et al., 1985; Dassori et al., 1987).

Results and Discussion

We divide our analysis into two sections. First we present the results for the general problem in terms of the dimensionless variables, then we use the model to analyze the experimental data for SO_2 removal with CuO.

To begin, we compare the behavior of single pellets with the same initial inert structure, but with different types of active solid distributions along the radius of the pellet, and with different values of the molal volume ratio C_v.

The radial distribution of active solid is fixed by the variation of the active to inert solid weight ratio W', and the method used ensures that the same mass of active solid is involved for a prescribed overall active solid weight fraction $\overline{W}_f$. Nevertheless, even though W' satisfies Eq. 45 it does not follow that all volume-averaged parameters are independent of the way in which solid is distributed for the same global active solid weight fraction.

In particular, the characteristic initial effective diffusivity, $\bar{D}_{e_o}$, when obtained by averaging D_{e_o} over the pellet volume, is dependent on the $W'(r)$ functionality, because of the general expression for D_e, Eq. 31. This means that for a fixed inert structure and prescribed active solid weight fraction, different active solid distributions give rise to slightly different ϕ^* and N values, because both of them depend upon $\bar{D}_{e_o}$. For calculational purposes, we have split each of those parameters into two terms: one constant, dependent only on properties not related to $W'(r)$ and another dependent on $\bar{D}_{e_o}$, which can be calculated for each $W'(r)$.

For the case of N:

$$N = N_1 N_2 \tag{48}$$

where

$$N_1 = R_p^2 M_B C_A^o bk/\rho_B r_o \tag{49}$$

$$N_2 = 1/\bar{D}_{e_o} \tag{50}$$

N_1 can be calculated from the set of physical properties of the system, while N_2 is known once $W'(r)$ has been chosen. The same can be done with ϕ^*:

$$\phi^* = \phi_1^* \phi_2^* \tag{51}$$

where

$$\phi_1^* = R_p S_i (k r_o/2\epsilon^*)^{1/2} \tag{52}$$

$$\phi_2^* = 1/(\bar{D}_{e_o})^{1/2} \tag{53}$$

The result is that the values of N and ϕ^* will vary slightly (<0.22%) for the solid distributions used in this work, for the same global weight fraction of solid.

Equation 33 can also be split for computational purposes using Eqs. 43 and 44 as:

$$D_K = D_{K_1} D_{K_2} \tag{54}$$

$$D_{K_1} = \frac{19{,}400\sqrt{T/M_A}\,\epsilon^*}{S_i} \tag{55}$$

$$D_{K_2} = \frac{f_p r_p^{*2} + 1 - f_p}{f_p r_p^* + 1 - f_p} \tag{56}$$

The active solid distribution, shown in Figure 2, was represented by two analytical expressions:

$$W'(r) = SR + 1 - 0.75S \tag{57}$$

for $S = 0$ and $S = 1$, and

$$W'(r) = \frac{S+3}{3} R^S \tag{58}$$

for $S = 2$ to $S = 22$.

We analyzed the case of three different weight fractions of active solid (0.05, 0.10, 0.15), holding ϕ_1^* and N_1 constant ($\phi_1^* = 1.0733\ s^{1/2}/cm$ and $N_1 = 1.8430 \times 10^{-4}\ cm^2/s$) so that the inert structure is preserved. The variation in the weight fraction makes ϕ^* and N vary slightly because of the variation of $\bar{D}_{e_o}$ for each case. Complete coverage of the inert solid surface is assumed; that is, $f_a = 1$. The variables that are kept constant for all of this part of the analysis are $D_M = 0.55\ cm^2/s$, $D_{K_1} = 0.01258\ cm^2/s$, $\rho_B/\rho_i = 6.4$, $Bi = 1$, $C_i = 0$, $\epsilon^* = 0.4$; these have been selected as typical for SO_2 removal with CuO (Yates and Best, 1976; Yeh et al., 1982). For this set of data diffusional resistance is expected to be important. Otherwise, active solid distributions would not make any difference in the results.

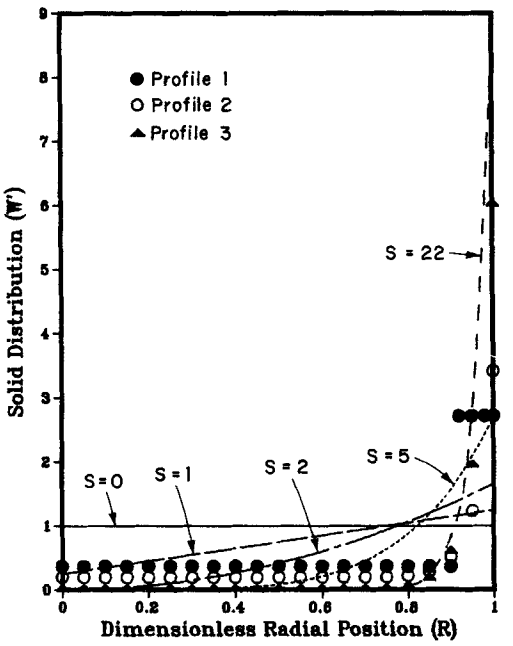

Figure 2. Active solid distribution in pellet.
Profile 1: $W' = 0.362$ if $R \le 0.9$, $= 2.716$ if $R > 0.9$
Profile 2: $W' = 0.193 + 3.221 * R^{22}$
Profile 3: $W' = 0.072 + 6.008 * R^{22}$
Other profiles as stated in text

The results for $\bar{W}_f = 0.05$ in the range of $C_v = 1$ to $C_v = 3$ show that the conversion profiles nearly overlap. Nevertheless, even at low active solid weight fractions ($\bar{W}_f = 0.05$), there is an important difference in the conversion vs. time relationship for different active solid distributions.

Figures 3 and 4 show the effect of increasing the weight fraction of active solid to 0.10 and 0.15, respectively. The effect of C_v is more noticeable as the weight fraction becomes larger. Differences up to 10–15% are found by comparing conversions for the same value of S. In Figure 4 differences up to 15–20% can be found for different C_v values. This increased importance of the molal volume ratio C_v is due to the existence of more active solid mass capable of disturbing the system.

The partial coverage profiles are shown in Figure 5 and the effect of partial coverage of the inert support is shown in Figure 6. The larger the ζ/r_o value, the lower the fractional solid conversion for a given dimensionless time. This difference grows as C_v increases. For $\zeta/r_o = 0.20$, with $C_v = 3$ and $S = 5$, Figure 6b, the leveling off of the reaction is caused by the blockage of active pores. Active solid material in those pores cannot react to completion because of this pore plugging. Pore plugging also happens for $\zeta/r_o = 0.20$, $C_v = 3$, and $S = 0$, but because of the even

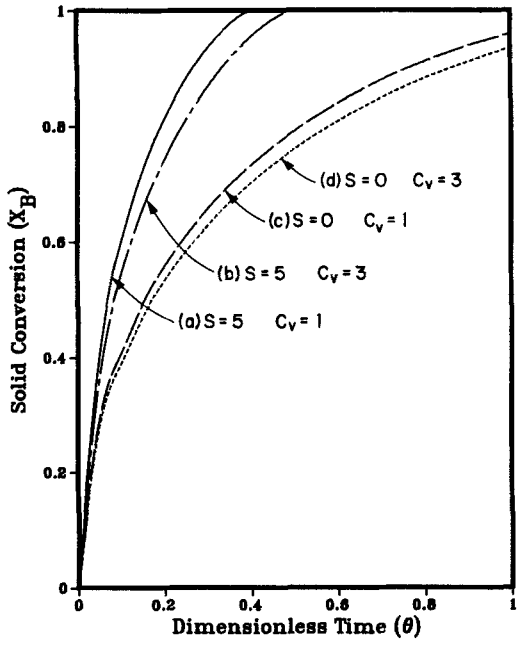

Figure 3. Solid conversion vs. dimensionless time for various active solid distributions.

(a) $\overline{W}_f = 0.1$; $\phi^* = 24.989$; $N = 0.099916$
(b) $\overline{W}_f = 0.1$; $\phi^* = 24.989$; $N = 0.099916$
(c) $\overline{W}_f = 0.1$; $\phi^* = 25.000$; $N = 0.1$
(d) $\overline{W}_f = 0.1$; $\phi^* = 25.000$; $N = 0.1$

distribution ($S = 0$) it takes longer to reach the point where complete blockage of active pores takes place. In the case of partial coverage of the inert matrix, pore plugging does not mean that the gas reactant cannot enter the pellet, because there is a

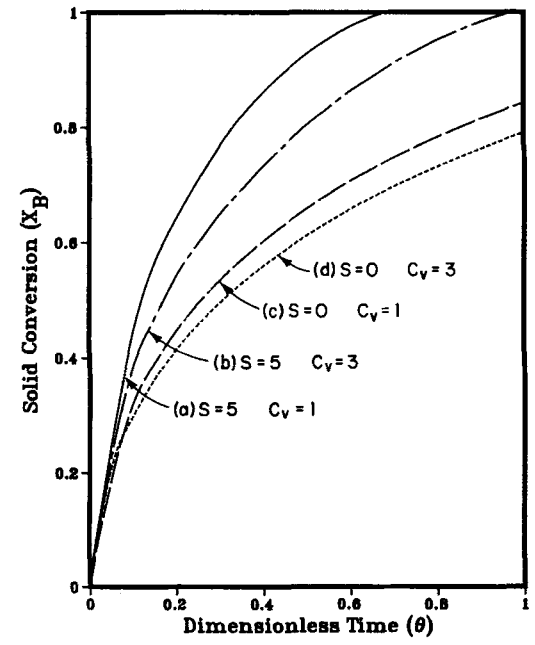

Figure 4. Solid conversion vs. dimensionless time for various active solid distributions.

(a) $\overline{W}_f = 0.15$; $\phi^* = 25.470$; $N = 0.10380$
(b) $\overline{W}_f = 0.15$; $\phi^* = 25.470$; $N = 0.10380$
(c) $\overline{W}_f = 0.15$; $\phi^* = 25.498$; $N = 0.10403$
(d) $\overline{W}_f = 0.15$; $\phi^* = 25.498$; $N = 0.10403$

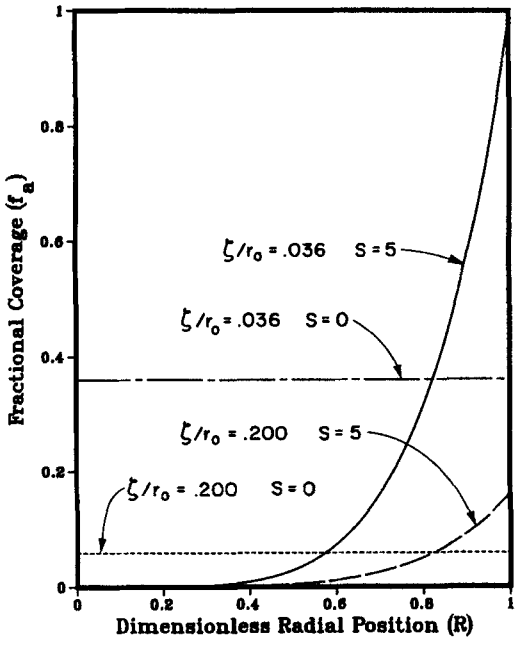

Figure 5. Fractional coverage f_a.
$\overline{W}_f = 0.1$

fraction of inert pores to flow through. An increase in ζ/r_o diminishes, for a fixed weight fraction $\overline{W}_f$, the coverage of the support. But one has to use large ζ/r_o values before obtaining significant variations in X_B. This means that for small values of ζ/r_o and nearly complete coverage of the support, this effect is of minor importance.

Application of model to SO_2 removal by CuO

We now use the present model to analyze SO_2 removal with impregnated CuO on alumina pellets. Data obtained from Yeh et al. (1982) and the physical properties of the system, as well as values for some estimated variables are reported in Table 1. The rate-controlling step for the process is stated by Yeh et al. to be:

$$CuO + SO_2 + \tfrac{1}{2} O_2 = CuSO_4$$

The oxygen concentration in the process is greatly in excess of the SO_2 concentration, and the oxygen concentration variation in the flue gas was found experimentally to have no effect on CuO conversion. Yeh et al. have determined experimentally that the rate of reaction is first order with respect to SO_2 concentration. Therefore, a first-order kinetics in SO_2 concentration inside the pores of the pellet and CuO surface area can be used, resulting in an expression for the rate of reaction per pore similar to Eq. 19.

Kinetic data have been reported by Yeh et al. (1982) for three different temperatures. We used several active solid distributions and compared their ability to represent the experimental data at the three temperatures reported. The profiles used in this work are depicted in Figure 2. We used an even distribution ($S = 0$), two different power functions ($S = 5, 22$) and three profiles, identified as *1*, *2*, and *3* in Figure 2. These latter were introduced to have an even distribution in the core of the pellet and a sharp increase toward the outer edge. Complete coverage

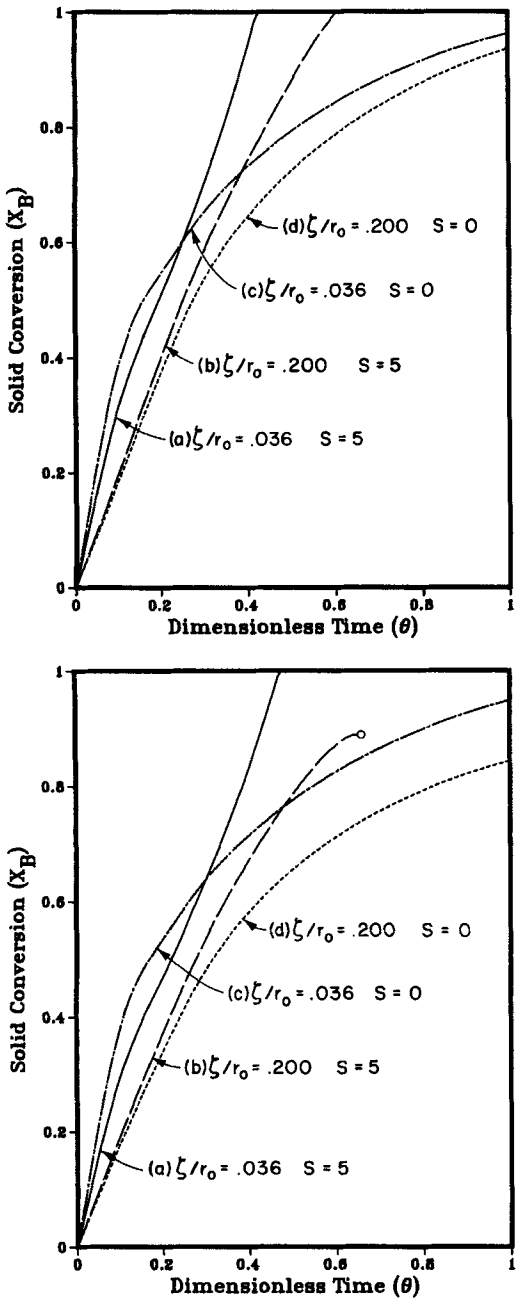

Figure 6. Effect of ζ/r_o on solid conversion for two molal volume ratios.

(a) $\phi^* = 24.988$; $N = 0.099906$
(b) $\phi^* = 24.974$; $N = 0.099791$
(c) $\phi^* = 24.998$; $N = 0.099985$
(d) $\phi^* = 24.983$; $N = 0.099865$

Figure 6a. $C_v = 1$; $\overline{W}_t = 0.1$.
Figure 6b. $C_v = 3$; $\overline{W}_t = 0.1$.

of the inert solid surface by the CuO was assumed. It is likely that CuO does not cover the entire inert matrix and therefore the surface coverage factor f_a should be smaller than one. But in the absence of appropriate experimental information to quantify this, we assumed $f_a = 1$ for the present analysis. The Biot number was fixed at $Bi = 1$. This is a lower bound and was constant because it was found that solid conversion was not sensitive to higher values. It was also assumed that the porosity of the solid product was very low when estimating the molal volume ratio C_v (= 3.6).

Table 1. Properties of the SO_2-CuO System

Active solid weight fraction (as Cu) = 5.6%
Pellet radius, R_p = 0.0795 cm
Alumina pellet porosity, ϵ^* = 0.5
Surface area per unit volume of alumina pellet, $S_i = 1.05 \times 10^6 \cdot cm^{-1}$
Alumina pellet density = 0.5 g/cm^3
SO_2 molecular weight = 64.07 g/mol
CuO molecular weight = 79.54 g/mol
$CuSO_4$ molecular weight = 159.61 g/mol
CuO density = 6.40 g/cm^3
$CuSO_4$ density = 3.61 g/cm^3
SO_2 partial pressure = 0.0027 atm
Molecular diffusion coefficient for SO_2, estimated for SO_2 in N_2 according to Fuller, Schettler, and Giddings relation (Perry and Green, 1984):
T = 350°C, D_M = 0.48 cm^2/s
T = 400°C, D_M = 0.55 cm^2/s
T = 450°C, D_M = 0.62 cm^2/s

Figures 7 and 8 show the results for the two extreme temperatures for which data were reported. The figures also show the mean relative deviation (MRD in the data) of the best fit for each profile, as well as the best value of the kinetic constant. We also present in each figure the result predicted by the macroscopic expression proposed by Yeh et al. (1982) to correlate their experimental data. For the set of trial profiles over the

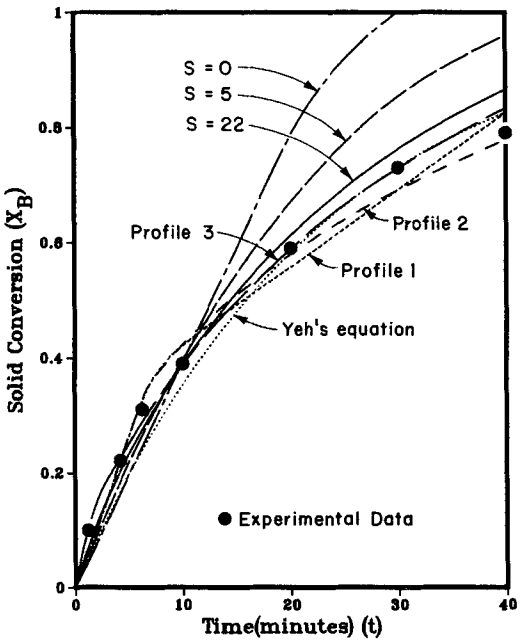

Figure 7. Comparison with experimental data at 350°C.

	k, cm/s	MRD,%
$S = 0$	5.80×10^{-6}	28.39
$S = 5$	7.50×10^{-6}	18.45
$S = 22$	1.75×10^{-5}	9.52
Profile		
1	7.47×10^{-6}	9.63
2	4.45×10^{-6}	8.76
3	1.09×10^{-5}	2.60
Yeh et al. (1982) eq.	—	12.52

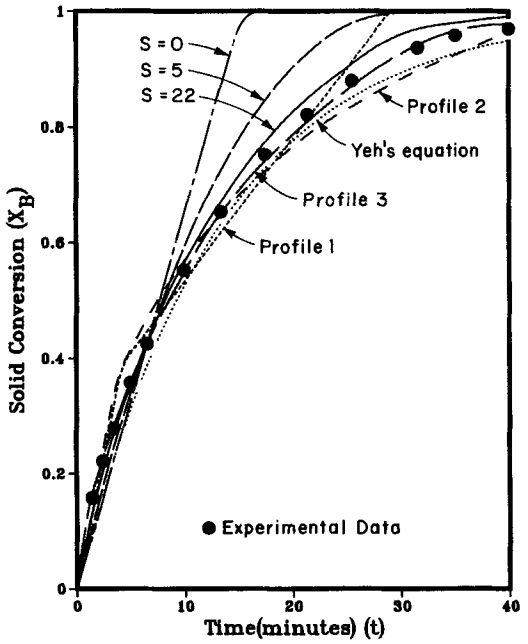

Figure 8. Comparison with experimental data at 450°C.

	k, cm/s	MRD,%
$S = 0$	1.15×10^{-5}	18.13
$S = 5$	1.48×10^{-5}	10.73
$S = 22$	3.59×10^{-5}	4.08
Profile		
1	1.59×10^{-5}	6.57
2	9.98×10^{-6}	7.21
3	2.24×10^{-5}	1.15
Yeh et al. (1982) eq.	—	5.84

three temperature values considered, it is clearly seen that some degree of sharp nonuniformity in the CuO profile is required in order to obtain a good fit of the experimental data. When considering the power law profiles ($S = 5, 22$) it is seen that an increase in S values produces a better fit of the data. However, other profiles that present a certain degree of uniformity mixed with a sharp increase close to the outer edge of the pellet (profiles *1*, *2*, and *3*) present the same or even better performance. Profile *1* shows a good behavior if one considers its mean relative deviation over the time span considered, but in contrast to profiles *2* and *3* it overpredicts solid conversion for higher values of time. Visual observations (Yeh, 1987, personal communication) indicate a largely uniform solid distribution inside the pellets, but with a sharp increase close to the outer edge of the pellet. Indeed, the three profiles considered show a better fit over the temperature and time range considered than the equation by Yeh et al. (1982), and one, profile *3*, becomes the best of all the profiles tried in this work. Nevertheless, the goodness of any profile must not be evaluated only on the basis of the mean relative deviation, but also on the way it fits the experimental evidence of the active solid distribution. As this effect was not quantified, no further comparison can be attempted, but it seems to be clearly shown that all three profiles meet both requirements very well. The behavior of the uniform active solid distribution ($S = 0$) is clearly the worst for the three temperatures considered. The model developed by Yeh et al. to correlate their data fits the data points well, despite the fact that internal processes inside the pellet are not included. Nevertheless, it does not take into account the weight fraction of active solid for estimating the kinetic constant, so results are valid for only one weight fraction. As was previously discussed, the variation of weight fraction, holding all other variables fixed, has a remarkable effect on the pellet performance, and it can not be excluded as an independent variable.

Some experiments were also done for higher active solid weight fractions (18% Cu), but the pellets had a tendency to break during the course of reaction (Yeh et al., 1987). This is additional evidence of the importance of structural changes, especially when working with moderately high active solid weight fractions. The breakage of the pellets can be ascribed to the tendency of the solid product to swell, because of the high molal volume ratio, C_v, of the system. As discussed when referring to Figures 3 and 4, the importance of structural changes within the pellet is amplified when the active solid weight fraction increases.

Conclusions

A pore-pellet model has been presented to account for nonuniform active solid distribution in gas-solid reactions in the presence of structural changes during the course of reaction. This model is particularly suitable for the study of SO_2 removal with CuO impregnated on alumina. The molal volume ratio, C_v, is an important variable for measuring the importance of structural changes, its influence being dependent on the weight fraction of active solid, $\overline{W_f}$. As expected, for the extreme case of very dilute active solid, structural changes are of minor importance. As the relative amount of solid reactant increases structural changes need to be considered.

The best performance of the pellet, in the absence of pore plugging, is found when the part richest in active solid is closest to the outer edge of the pellet. The case of an unevenly distributed active solid with uniform thickness was also considered and it was found that a new feature, the partial coverage ($f_a < 1$), is needed. It is shown that C_v and ζ/r_o values have to be relatively high and active solid distribution has to be steep, in order to differ significantly from the complete coverage case.

The ability of the present model to fit experimental data has been tested using data for SO_2 removal with CuO impregnated on alumina. It was necessary to resort to some degree of nonuniformity in the active solid distribution in order to get the best fit of literature data, in agreement with reported evidence of nonuniformity (Yeh, 1987, personal communication). In contrast with a previous model for the same system (Yeh et al., 1982), this model characterizes the kinetic process by a kinetic constant that is independent of the active solid weight fraction. In the case of dilute active solid pellets, such as SO_2 removal with CuO, the active solid weight fraction has to be considered as an independent model variable for obtaining kinetic constants that can be extrapolated to pellets with other active solid weight fractions.

Acknowledgment

The authors are grateful to Consejo Nacional de Investigaciones Cientificas y Tecnicas de la Republica Argentina for a fellowship to C. G. Dassori that made this research possible.

Notation

A_i = surface area of reaction front
A_p = surface area of pore

b = stoichiometric coefficient of B
Bi = Biot number, D_e/kr_o
C = nondimensional gas reactant concentration, C_A/C_A^o
C^* = nondimensional initial gas reactant concentration inside pellet, C_A^*/C_A^o
C_A = gas reactant concentration
C_A^* = initial gas concentration inside pellet
C_A^o = bulk gas concentration
C_{Ai} = gas reactant concentration at reaction front
C_v = coefficient, Eq. 23
D_e = effective diffusivity of gas reactant through pores of pellet
D_{e_o} = effective diffusivity of gas reactant through pores of pellet at $t = 0$
$\bar{D}_{e_o}$ = volume-averaged value of D_{e_o}, $\int_0^1 R^2 D_{e_o} dR$
D_K = Knudsen diffusion coefficient of reactant A
D_{K_1} = coefficient, Eq. 55
D_{K_2} = coefficient, Eq. 56
D_M = molecular diffusion coefficient of reactant A
D_s = effective diffusivity of gas reactant through product layer
f_a = surface coverage factor
f_p = fraction of active pores
g = stoichiometric coefficient of G
k = kinetic constant
l = mean pore length
M_A = molecular weight of A
M_B = molecular weight of B
M_G = molecular weight of G
$N = R_p^2 M_B C_A^o bk/\rho_B r_o \bar{D}_{e_o}$
N_1 = factor, Eq. 49
N_2 = factor, Eq. 50
N_p = number of pores per unit volume
n_A = number of moles of reactant A
r = radial coordinate in pellet, dimensional
r_B = rate of disappearance of reactant B
r_i^* = nondimensional radius of reaction front, r_i/r_o
r_i = radius of reaction front
r_p = radius of pore
r_p^* = nondimensional radius of pore, r_p/r_o
r_o = mean pore radius
R = nondimensional radial coordinate in pellet, r/R_p
R_p = pellet radius
S = surface area per unit volume of pellet under reaction conditions
S_i = surface area of inert support per unit volume
S^o = surface area per unit volume after impregnation
$\bar{S}^o$ = volume-averaged value of S
t = time, dimensional
T = temperature of pellet
W = active to inert solid weight ratio
$\bar{W}$ = volume-averaged value of W
$W' = W/\bar{W}$
$\bar{W}_f$ = weight fraction of active solid
X_B = fractional conversion of solid B

Greek letters

$\delta = D_e/\bar{D}_{e_o}$
ϵ = porosity of pellet under reaction conditions
ϵ_G = porosity of product layer
ϵ^* = porosity of inert support
ϵ^o = porosity of impregnated pellet
$\bar{\epsilon}^o$ = volume-averaged value of ϵ^o
θ = nondimensional time $= tM_B C_A^o bk/\rho_B r_o$
ρ_B = density of reactant B
ρ_G = density of reactant G
ρ_i = density of inert support
$\phi^* = R_p S_i (kr_o/2\epsilon^* \bar{D}_{e_o})^{1/2}$
ζ = active solid layer thickness

Literature Cited

Dassori, C. G., J. W. Tierney, and Y. T. Shah, "Transient Analysis of the Particle-Pellet Model with Structural Changes in the Solid Phase," *Reactions and Reaction Engineering*, R. A. Mashelkar and R. Kumar, eds., Indian Acad. Sciences, Bangalore (1987).

Doraiswamy, L. K., and M. M. Sharma, *Heterogeneous Reactions: Analysis, Examples, and Reactor Design*, **1**, Wiley, New York (1984).

Dudukovic, M. P., "Reactions of Particles with Nonuniform Distribution of Solid Reactant. The Shrinking Core Model," *Ind. Eng. Chem. Process Des. Dev.*, **23**, 330 (1984).

Hindmarsh, A. C., "LSODE and LSODI, Two New Initial Value Ordinary Differential Equation Solvers," *ACM SIGNUM Newsl.*, **15**, 10 (1980).

Johnson, S. H., and A. C. Hindmarsh, "Numerical Dynamic Simulation of Solid-Fluid Reactions in Isothermal Porous Spheres," *J. Comp. Phys.*, **52**, 503 (1983).

Perry, R. H., and D. W. Green, *Chemical Engineers Handbook*, McGraw-Hill, New York, 3-285 (1984).

Prasannan, P. C., P. A. Ramachandran, and L. K. Doraiswamy, "A Model for Gas-Solid Reactions with Structural Changes in the Presence of Inert Solids," *Chem. Eng. Sci.*, **40**, 1251 (1985).

Ramachandran, P. A., and L. K. Doraiswamy, "Modeling of Noncatalytic Gas-Solid Reactions," *AIChE J.*, **28**, 881 (1982).

Ramachandran, P. A., and M. P. Dudukovic, "Reactions of Solid Particles with Nonuniform Distribution of Solid Reactant. The Volume Reaction Model," *Chem. Eng. Sci.*, **39**, 669 (1984).

Ramachandran, P. A., and J. M. Smith, "Effect of Sintering and Porosity Changes on the Rate of Gas-Solid Reactions," *Chem. Eng. J.*, **14**, 137 (1977).

Satterfield, C. N., *Mass Transfer in Heterogeneous Catalysis*, MIT Press, Cambridge, MA (1970).

Sohn H. Y., and Y-N. Xia, "Effect of Nonuniform Distribution of Solid Reactant on Fluid-Solid Reactions. 1: Initially Nonporous Solids," *Ind. Eng. Chem. Process Des. Dev.*, **25**, 386 (1986).

———, "Effect of Nonuniform Distribution of Solid Reactant on Fluid-Solid Reactions. 2: Porous Solids," *Ind. Eng. Chem. Res.*, **26**, 246 (1987).

Sohn, H. Y., S. H. Johnson, and A. C. Hindmarsh, "Application of the Method of Lines to the Analysis of Single Fluid-Solid Reactions in Porous Solids," *Chem. Eng. Sci.*, **40**, 2185 (1985).

Yates, J. G., and R. J. Best, "Kinetics of Reaction between Sulfur Dioxide, Oxygen, and Cupric Oxide in a Tubular, Packed Bed Reactor," *Ind. Eng. Chem. Process Des. Dev.*, **15**, 239 (1976).

Yeh, J. T., R. J. Demski, and J. I. Joubert, "SO_2 Absorption and Regeneration Kinetics Employing Supported Copper Oxide," *AIChE Summer Nat. Meet.*, Cleveland (1982).

Yeh, J. T., C. J. Drummond, and J. I. Joubert, "Process Simulation of the Fluidized-Bed Copper Oxide Process Sulfation Reaction," *Environ. Prog.*, **6**, 44 (1987).

Manuscript received Nov. 6, 1987, and revision received June 7, 1988.